Journal of Catalysis **198,** 122–127 (2001)
doi:10.1006/jcat.2000.3105, available online at http://www.idealibrary.com on IDEAL®

Tuning the Selectivity of Acetylene Polymerization Atom by Atom

Stéphane Abbet, Antonio Sanchez, Ueli Heiz,[1] and Wolf-Dieter Schneider

Institut de Physique de la Matière Condensée, Université de Lausanne, CH-1015 Lausanne, Switzerland

Received August 24, 2000; revised October 27, 2000; accepted October 27, 2000; published online February 1, 2001

The polymerization of acetylene was studied by thermal programmed reaction on nanoassembled model catalysts fabricated by soft landing of size-selected palladium Pd_n ($1 \leq n \leq 30$) clusters on well-characterized MgO(100) thin films. In a single-pass heating cycle experiment, benzene, butadiene, and butene were catalyzed with different selectivities as a function of cluster size: palladium atoms selectively produce benzene, and the highest selectivity for butadiene is observed for Pd_6, whereas Pd_{20} reveals the highest selectivity for butene. These results provide an atom-by-atom observation of the selectivity of small palladium model catalysts, and extend toward small cluster sizes the study of Ormerod and Lambert on real palladium catalysts, where a structure sensitivity for the cyclotrimerization was observed.

Key Words: **palladium clusters; magnesium oxide films; selectivity; acetylene polymerization; size effects; size-selected clusters; model catalysts.**

1. INTRODUCTION

Microscopic insight into important catalytic reactions (1, 2) has been gained on single crystal surfaces (3–5). However, in general, industrial catalysts consist of small metal particles supported on oxides where the particle size plays an important role in determining the catalytic properties (6). In a size range of hundreds to thousands of atoms the surface morphology of the particles governs the kinetics and the selectivity of reactions (7–11). For nanoclusters containing only a few atoms quantum size effects become dominant and an understanding of their size-dependent catalytic activity is emerging (12–17). The polymerization of acetylene over supported Pd particles reveals a direct correspondence between reactivities observed on model systems and the behavior of industrial catalysts under working conditions (7). In ultrahigh vacuum (UHV) (8) as well as under high pressure, large palladium particles of typically thousands of atoms show an increased selectivity for the formation of benzene with increasing particle size (7). In contrast, small palladium particles of typically hundreds of atoms are less selective for the cyclotrimerization and catalyze butadiene and butene as additional products (7). So far, however, information on the atom-by-atom evolution of this astonishing catalytic selectivity is still lacking. Motivated and challenged by the prevailing opinion that "it is virtually impossible to prepare a collection of metallic particles that is truly monodispersive (i.e., where all have exactly the same size)" (18), we succeeded in the polymerization of acetylene to prepare nanoassembled model catalysts consisting of size-selected Pd_n ($1 \leq n \leq 30$) clusters supported on thin MgO films. We observed for the first time a striking atom-by-atom size-dependent selectivity for the reaction paths toward the formation of butadiene, butene, and benzene.

[1] To whom correspondence should be addressed. Fax: +41 21 693 3604. E-mail: Heiz@dpmail.epfl.ch.

2. MODEL CATALYST PREPARATION AND CHARACTERIZATION

Monodispersed cluster ions, selected from a distribution of cluster sizes obtained by supersonic expansion of a cold (40 K) laser-generated metal plasma, were deposited using the experimental scheme shown in Fig. 1. Most of the total deposition energy, being smaller than the binding energies of the investigated Pd clusters (17, 19), is rapidly dissipated via the solid surface (20). Therefore, under these conditions the clusters soft-land (that is, without fragmentation) on the substrate (20–22). Soft landing of the clusters on the oxide supports is also suggested by first principle calculations where Au_8 is deposited on various MgO surfaces, showing that the cluster's structure is only slightly distorted in comparison to the gas phase (16). That clusters indeed maintain their identity upon deposition is also shown experimentally. The carbonyl formation of small deposited Ni_n ($n = 1$–30) was studied by exposing the deposited clusters to carbon monoxide (14). These mass spectrometry experiments showed that the nuclearity of the formed Ni_n carbonyls ($n = 1$–3) is not changed. The absence of, for example, $Ni(CO)_4$ and $Ni_3(CO)_x$ after deposition of Ni_2 directly indicates that fragmentation upon deposition can be excluded under our experimental conditions. Deposition of less than 1% of a monolayer (ML) of Pd clusters ($1\ \text{ML} = 2.2 \times 10^{15}$ clusters/cm^2) at a substrate temperature of 90 K assures the presence of isolated supported

0021-9517/01 $35.00

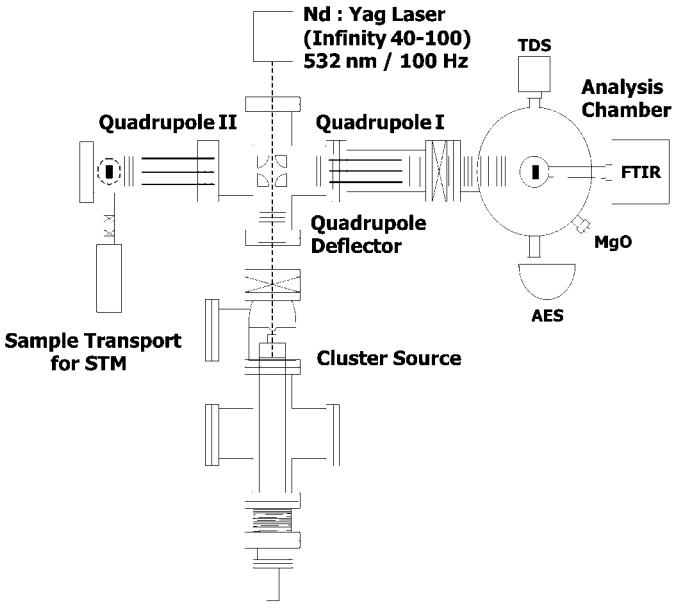

FIG. 1. Experimental setup. The clusters are produced by a laser evaporation source (cluster source). The cluster ions are guided with ion optics into a quadrupole mass spectrometer (quadrupole I). The size-selected clusters are deposited onto an *in situ* prepared MgO film. In the analysis chamber the size-dependent reactivities are studied by thermal desorption spectroscopy (TDS), Fourier transform infrared (FTIR) spectroscopy, and Auger electron spectroscopy (AES).

clusters pinned on the defect sites of the support (14–17, 23). The existence of monodispersed Pd_n clusters is proven by the excellent agreement of the measured vibrational frequencies and binding energies of CO on various cluster sizes with theoretical CO values (24). The support is prepared *in situ* by epitaxially growing thin MgO(100) films on a Mo(100) surface (25). These films show bulklike properties (23). Small amounts of defects such as steps, kinks, and F-centers are detected from the desorption behavior of small molecules (16, 26). To obtain identical conditions for the study of the polymerization on different Pd cluster sizes we first exposed, using a calibrated molecular beam doser, the prepared model catalysts at 90 K to an average of 1 Langmuir (L) of acetylene, corresponding to saturation coverage (27). In a temperature-programmed reaction (TPR) catalytically formed benzene (C_6H_6), butadiene (C_4H_6), and butene (C_4H_8) molecules are detected by mass spectrometry and monitored as functions of temperature and cluster size. The cluster reactivities were obtained by a single-pass heating cycle. The thermal stabilities of the deposited clusters were investigated by Fourier transform infrared (FTIR) spectroscopy for Pd atoms, which are found not to migrate up to around 350 K. Up to this temperature the vibrational frequency of adsorbed CO is not changing (17). This rather high stability can be explained by the high binding energy (~4 eV) of Pd atoms bound to the F-centers (28). For clusters the binding energy is expected to be even

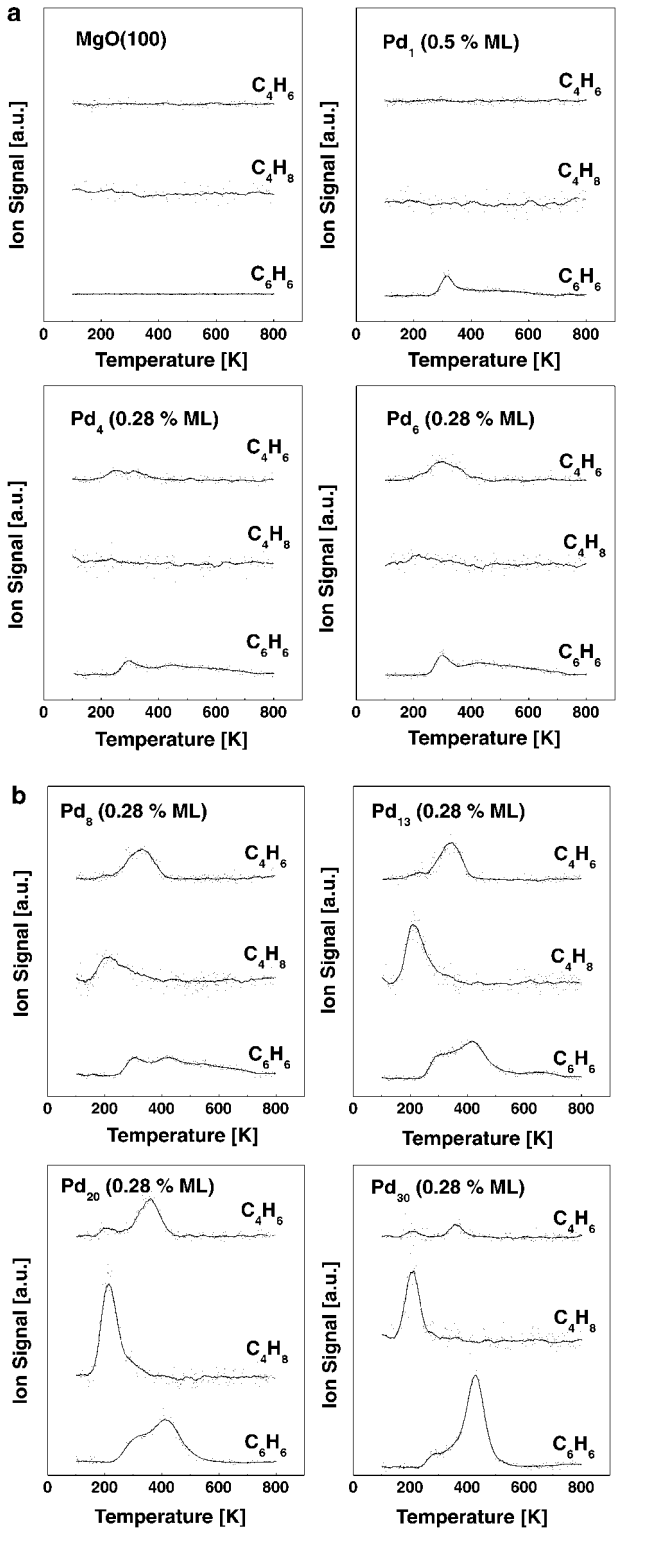

FIG. 2. (a) TPR spectra of the catalytic formation of C_6H_6, C_4H_8, and C_4H_6 for Pd_1, Pd_4, and Pd_6. Note that clean MgO thin films do not catalyze the formation of these products. (b) TPR spectra of the catalytic formation of C_6H_6, C_4H_8, and C_4H_6 for Pd_8, Pd_{13}, Pd_{20}, and Pd_{30}. The relative ion intensities are corrected with the relative detection efficiencies of the experiment and scale with the number of formed product molecules per cluster.

higher and therefore migration is unlikely. Upon heating, different isomers may be present on the surface. This behavior has not yet been studied in detail. In the case of Au_8 adsorbed on F-centers of a MgO thin film, however, we have shown the reactivity not to change even after several reaction cycles (16).

3. ATOM-BY-ATOM SIZE-DEPENDENT SELECTIVITY

The TPR spectra of the different products of the polymerization of acetylene, obtained in a *single-pass heating cycle*, on small supported, monodispersed palladium clusters and on the bare MgO films are shown in Figs. 2a and 2b. As expected, the oxide support does not catalyze the polymerization reaction. However, as soon as palladium clusters are present, striking atom-by-atom size-dependent reactivities and selectivities are observed. Only the three reaction products C_6H_6, C_4H_8, and C_4H_6 are detected. They are unambiguously characterized by their fragmentation patterns. Remarkably, no C_3H_n, C_5H_n, and C_8H_n are formed,

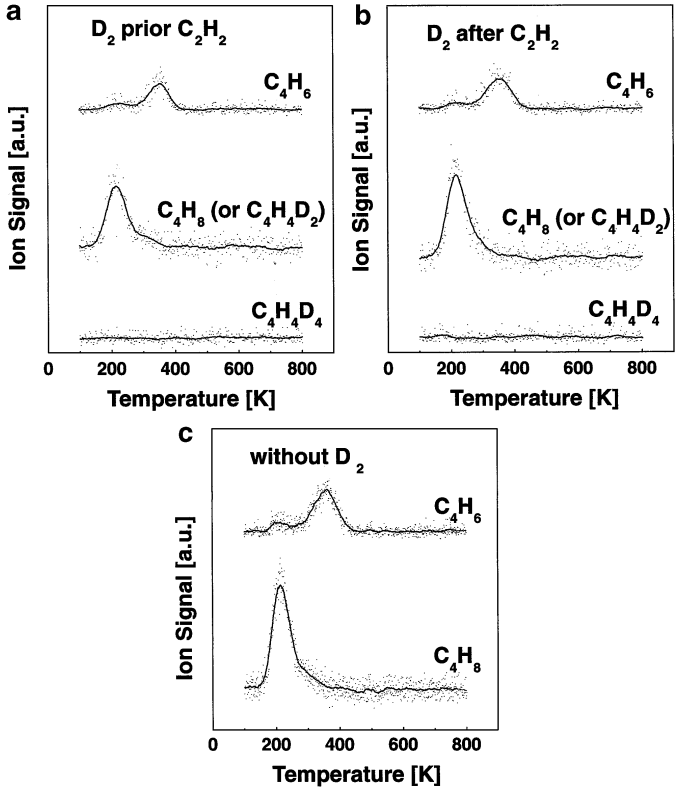

FIG. 3. (a) Polymerization of acetylene after saturating the model catalysts (Pd_{20}/MgO) with D_2. Note that no products containing deuterium are produced. The formation of $C_4H_4D_2$ (having the same mass as C_4H_8) is excluded, as no desorption of this mass is observed around 350 K. However, the reactivity is slightly decreased when compared with the reactivity of the model catalysts not exposed to D_2 (c). (b) Polymerization of acetylene on the model catalysts (Pd_{20}/MgO) when it is exposed to D_2 after saturation of C_2H_2. No products containing deuterium are produced.

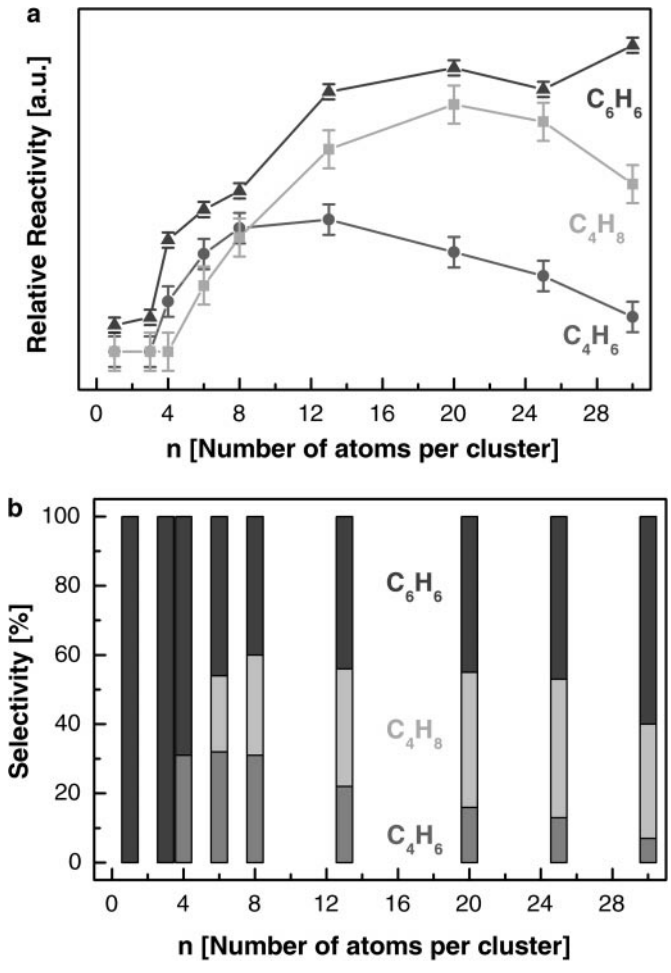

FIG. 4. (a) Cluster size-dependent reactivity expressed as the relative number per cluster of formed product molecules, C_6H_6, C_4H_8, and C_4H_6. Maximal reactivity for the formation of C_4H_6 for cluster sizes around Pd_{10}; for the formation of C_4H_8 for cluster sizes around Pd_{20}, the formation of C_6H_6 is increasing with size. (b) Size-dependent selectivity in % for the polymerization of acetylene (see text). Pd_{1-3} show 100% selectivity for the cyclotrimerization, whereas the selectivity for the hydrogenation of the intermediate (C_4H_4) to C_4H_6 (30%) and C_4H_8 (~40%) is maximal for Pd_6 and Pd_{20-25}, respectively.

indicating the absence of C–C bond scission as already observed on Pd single crystals (29) and Pd particles (7). Up to Pd_3, only benzene is catalyzed, reflecting a high selectivity for the cyclotrimerization of acetylene (30). Pd_n ($4 \leq n \leq 6$) clusters reveal a second reaction channel by catalyzing in addition C_4H_6, which desorb around 300 K. The third reaction product, C_4H_8, desorbing at a rather low temperature of 200 K, is clearly observed for Pd_8. For this cluster size the abundance of the three reaction products is similar. For even larger clusters ($13 \leq n \leq 30$) the formation of C_6H_6 increases with cluster size, whereas the conversion of acetylene into C_4H_8 reaches a maximum for Pd_{20}. Note that Pd_{30} selectively suppresses the formation of C_4H_6. (The peak in the TPR spectrum of C_4H_6 at 200 K is part of the

fragmentation pattern of C_4H_8.) For Pd_{20} the experiments were repeated in the presence of D_2: D_2 was exposed before (Fig. 3a) and after (Fig. 3b) C_2H_2. For comparison the formation of C_4H_6 and C_4H_8 on Pd_{20} without the use of D_2 is also shown in Fig. 3c. The results clearly indicate that no product containing deuterium is formed. Consequently, D_2 is not involved in the polymerization reaction. However, the presence of D_2 opens a new reaction channel, the hydrogenation of acetylene. In addition, D_2 blocks the active sites on the palladium clusters for the polymerization, as the formation of the products is slightly reduced when exposing D_2 prior to C_2H_2. On Pd(111), predosing with H_2 completely suppresses the cyclotrimerization but enhances the hydrogenation of acetylene to form ethylene (31).

The relative ion intensities of the products in the TPR spectra scale with the product formation by the model catalysts (32). By integrating the total area of the TPR spectra shown in Figs. 2a and 2b, the number of catalytically produced benzene, butadiene, and butene molecules per cluster is obtained and illustrated in Fig. 4a. Figure 4b shows the selectivities S for the formation of the products P_1 (C_6H_6), P_2 (C_4H_6), and P_3 (C_4H_8) for different cluster sizes calculated from, e.g.,

$$S(P_1) = (\text{number of } P_1 \text{ per cluster/number of } \sum P_n \text{ per cluster}) \times 100 \quad (\%)$$

The striking atom-by-atom size-dependent selectivity for the polymerization of acetylene is summarized as follows: C_6H_6 is catalyzed with a selectivity of 100% on cluster sizes up to Pd_3. The selectivity for C_4H_6 reaches a maximum for Pd_6 (~30%) and the production of C_4H_8 is most efficient (~40%) for Pd_{20-25}.

4. PROPOSED REACTION MECHANISM

Analyzing the products formed on small size-selected Pd_n ($1 \le n \le 30$) clusters deposited on MgO(100) thin films indicates that the surface intermediate C_4H_4 is being produced efficiently on all cluster sizes. Thus, at least two acetylene molecules are adsorbed in a π-bonded configuration at the initial stage of the reaction (17). The observed

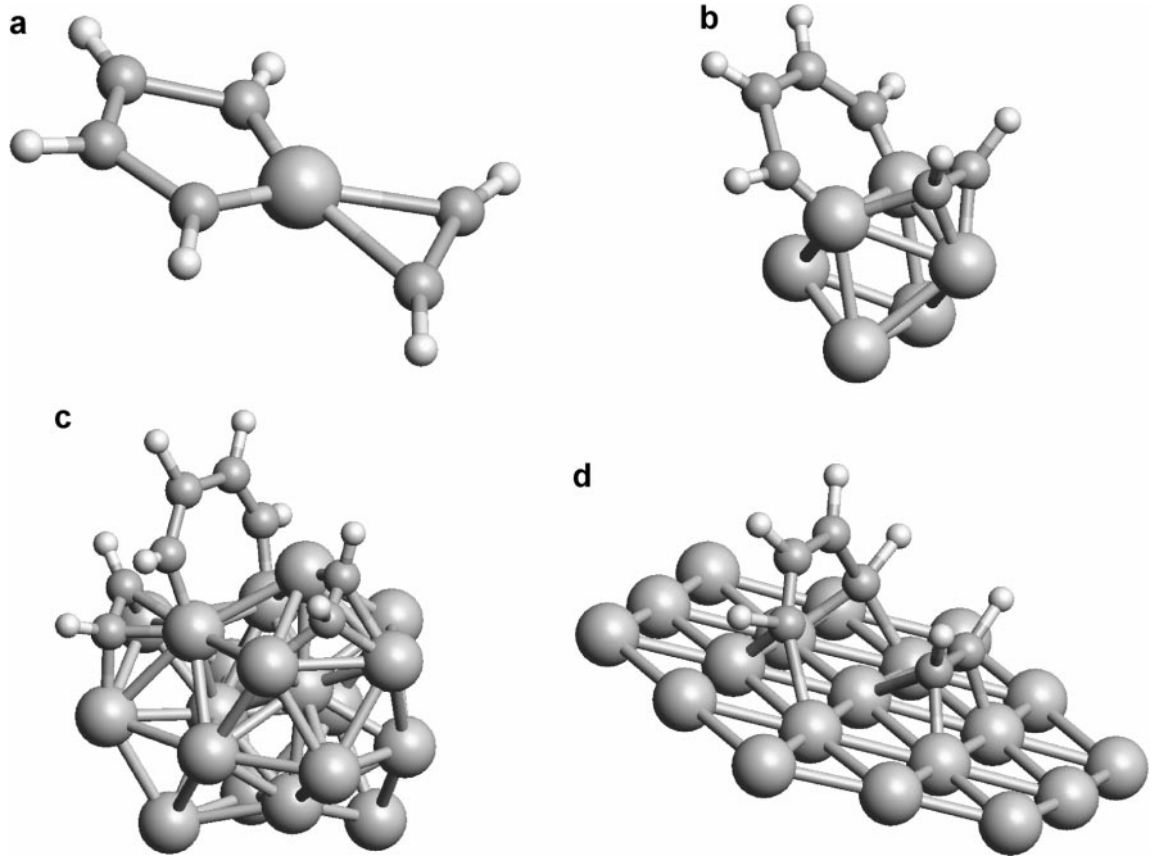

FIG. 5. Proposed structures of the complexes. (a) $Pd^{-0.6}$– (C_4H_4)(C_2H_2 π-bonded) (17); (b) Pd_6-(C_4H_4)(C_2H_2 di-σ/π-bonded), Pd_6 structure taken from (36); (c) Pd_{20}-(C_4H_4) 2(C_2H_2 di-σ/π-bonded), Pd_{20} structure (Morse cluster) taken from (37); and (d) Pd(111)-(C_4H_4)(C_2H_2 di-σ/π-bonded) (33). In this schematic representation the cluster structures were obtained from existing calculations. For Pd_6 and Pd_{20} the adsorption configurations of C_2H_2 and C_4H_4 are taken in analogy to the surface structures (33).

size-dependent selectivity may then be understood by regarding the influence of the cluster size to steer the reaction either toward the cyclotrimerization to form C_6H_6 or toward a direct hydrogen transfer from adsorbed C_2H_2 to the C_4H_4 intermediate to catalyze the formation of C_4H_6 or C_4H_8, respectively. Cyclotrimerization is generally observed when a third acetylene molecule is adsorbed in a π-bonded configuration, which results in a change from *sp* hybridization toward sp^2 hybridization (33). This bonding configuration leads to a weak activation of the C–H bond, in analogy to ethylene (34). The hydrogenation of the $Pd_n(C_4H_4)$ metallocycle, on the other hand, is favored by the adsorption of di-σ/π-bonded acetylene to three Pd atoms, effecting a more efficient activation of the C–H bond, in analogy to ethylene (34).

For Pd atoms adsorbed on defect sites the $Pd(C_4H_4)$ intermediate is formed with an energy gain of around 4 eV. A third adsorbed C_2H_2 molecule is purely π-bonded (Fig. 5a) and the activated acetylene molecule reacts with the intermediate to form benzene with a total exothermicity of about 7 eV. The weakly bound C_6H_6 (0.3eV) then desorbs at low temperatures from the model catalyst (17). A second reaction channel, the formation of butadiene, C_4H_6, opens for Pd_4. This channel reveals the highest selectivity for Pd_6; in this case a third C_2H_2 molecule can bind in a di-σ/π bond configuration to three Pd atoms (as shown in Fig. 5b). The charge transfer from the substrate to the cluster further enhances the activation of the C–H bonds. For even larger cluster sizes the adsorption of two di-σ/π-bonded C_2H_2 molecules becomes possible (Fig. 5c) and opens up the third reaction path, the formation of C_4H_8. In our experiments this is clearly observed for Pd_8. Purely geometrical arguments (possible adsorption of two di-σ/π-bonded C_2H_2 molecules close to the C_4H_4 intermediate) suggest that this third channel is more pronounced for the larger clusters, and indeed our results show maximal C_4H_8 formation for cluster sizes of 20–25 Pd atoms. For the largest clusters of the measured range, e.g., Pd_{30}, the increased number of metal–metal bonds and the concomitant delocalization of the charge transferred from the substrate to the cluster results in less charge density available for the activation of the C–H bond (35). Consequently, the cyclotrimerization becomes again more efficient than the hydrogenation of the C_4H_4 intermediate. On going to even larger particles or to Pd(111) single crystals the cyclotrimerization to benzene is selectively catalyzed (Fig. 5d). A deeper understanding of the observed size-dependent catalytic selectivity might only be possible with theoretical modeling of the reaction kinetics.

It is clear that still serious obstacles lie between what we have demonstrated and the realization of useful size-selected catalysts. The prospect of tuning atom by atom the activity and selectivity of real catalysts is nonetheless a little closer.

ACKNOWLEDGMENTS

This work has been supported by the Swiss National Science Foundation. U.H. acknowledges a fellowship from the Humboldt Foundation. We thank G. Pacchioni for very stimulating discussions.

REFERENCES

1. Ertl, G., Knözinger, H., and Weitkamp, J., "Handbook of Heterogeneous Catalysis." Wiley, New York, 1997.
2. Bond, G. C., "Heterogeneous Catalysis: Principles and Applications." Clarendon Press, Oxford, 1974.
3. Wintterlin, J., Völkening, S., Janssens, T. V. W., Zambelli, T., and Ertl, G., *Science* **278**, 1931 (1997).
4. Over, H., Kim, Y. D., Seitsonen, A. P., Wendt, S., Lundgren, E., Schmid, M., Varga, P., Morgante, A., and Ertl, G., *Science* **287**, 1474 (2000).
5. Besenbacher, F., Chorkendorff, I., Clausen, B. S., Hammer, B., Molenbroek, A. M., Norskov, J. K., and Stensgaard, I., *Science* **279**, 1913 (1998).
6. Boudard, M., *Adv. Catal.* **20**, 153 (1969).
7. Ormerod, R. M., and Lambert, R. M., *J. Chem. Soc., Chem. Commun.* 1421 (1990).
8. Holmblad, P. M., Rainer, D. R., and Goodman, D. W., *J. Phys. Chem. B* **101**, 8883 (1997).
9. Andersson, S., Frank, M., Sandell, A., Giertz, A., Brena, B., Bruehwiler, P. A., Martensson, N., Libuda, J., Bauemer, M., and Freund, H.-J., *J. Chem. Phys.* **108**, 2967 (1998).
10. Henry, C. R., *Surf. Sci. Rep.* **31**, 231 (1998).
11. Valden, M., Lai, X., and Goodman, D. W., *Science* **281**, 1647 (1998).
12. Fayet, P., Granzer, F., Hegenbart, G., Moisar, E., Pischel, B., and Woeste, L., *Phys. Rev. Lett.* **55**, 3002 (1985).
13. Xu, Z., Xiao, F.-S., Purnell, S. K., Alexeev, O., Kawi, S., Deutsch, S. E., and Gates, B. C., *Nature* **372**, 346 (1994).
14. Heiz, U., Vanolli, F., Sanchez, A., and Schneider, W.-D., *J. Am. Chem. Soc.* **120**, 9668 (1998).
15. Heiz, U., Sanchez, A., Abbet, S., and Schneider,W.-D., *J. Am. Chem. Soc.* **121**, 3214 (1999).
16. Sanchez, A., Abbet, S., Heiz, U., Schneider, W.-D., Häkkinen, H., Barnett, R. N., and Landman, U., *J. Phys. Chem. A* **103**, 9573 (1999).
17. Abbet, S., Sanchez, A., Heiz, U., Schneider, W.-D., Ferrari, A. M., Pacchioni, G., and Rösch, N., *J. Am. Chem. Soc.* **122**, 3453 (2000).
18. Bond, G. C., and Thompson, D. T., *Catal. Rev.-Sci. Eng.* **41**, 319 (1999).
19. The total energy of the deposition is composed of the kinetic energy of the cluster ($E_{kin} < 0.2$ eV/atom [see Ref. 22]) and the involved chemical binding energy between the cluster and the MgO surface (~0.3 eV per interacting atom for Pd_4 [see Yudanov *et al., Chem. Phys. Lett.* **275**, 245 (2000)], which is most probably higher when the cluster is directly deposited on an F-center), as well as a negligable Coulomb interaction of the incoming cluster ion and its induced polarization and image charge on the oxide film surface and in the metal, respectively. Consequently, as the kinetic energies of the impinging clusters correspond to soft landing conditions ($E_{kin} < 1$ eV [see Refs. 20, 21]) and as the total energy gain upon deposition is smaller than the calculated binding energies of the investigated Pd clusters (ranging from 1.4 to 3.9 eV for Pd_4 to bulk [see Moseler *et al., Phys. Rev. Lett.*, in press]), fragmentation of the clusters induced by the deposition alone is excluded.
20. Cheng, H.-P., and Landman, U., *J. Phys. Chem.* **98**, 3527 (1994).
21. Bromann, K., Felix, C., Brune, H., Harbich, W., Monot, R., Buttet, J., and Kern, K., *Science* **274**, 956 (1996).
22. Heiz, U., Vanolli, F., Trento, L., and Schneider, W.-D., *Rev. Sci. Instrum.* **68**, 1986 (1997).

23. Schaffner, M.-H., Patthey, F., Schneider, W.-D., and Pettersson, L. G. M., *Surf. Sci.* **450**, 402 (1998).
24. The experimental vibrational frequencies of adsorbed CO on supported Pd_n clusters (2055 cm^{-1} for Pd_1 and 2089 cm^{-1} for Pd_4) show distinct cluster size-dependent variations and are in good agreement with existent theoretical CO frequencies for Pd_1 (2054 cm^{-1}) and Pd_4 (2086 cm^{-1}) [see Neyman *et al., Appl. Catal. A* **191**, 3–13 (2000)].
25. Wu, M. C., Corneille, J. S., Estrada, C. A., He, J.-W., and Goodman, D. W., *Chem. Phys. Lett.* **182**(5), 472 (1991).
26. Heiz, U., and Schneider, W.-D., *J. Phys. D: Appl. Phys.* **33**, R85 (2000).
27. Under these conditions the clusters are saturated with C_2H_2 as desorption of physisorbed C_2H_2 from the MgO films is detected.
28. Ferrari, A. M., Giordano, L., Rösch, N., Heiz, U., Abbet, S., Sanchez, A., and Pacchioni, G., *J. Phys. Chem. B* **104**, 10612 (2000).
29. Patterson, C. H., and Lambert, R. M., *J. Phys. Chem.* **92**, 1266 (1988).
30. Recent *ab initio* calculations showed that from a purely thermodynamic point of view two isolated Pd atoms on MgO are more stable than an adsorbed dimer [see Ferrari *et al., Phys. Chem. Chem. Phys.* **1**, 4655 (1999)].
31. Tysoe, W. T., Nyberg, G. L., and Lambert, R. M., *J. Chem. Soc., Chem. Commun.* 623 (1983).
32. The mass spectrometer was calibrated for the three species using a flow-calibrated molecular beam doser and relative detection efficiencies of the three measured masses (78 for benzene, 56 for C_4H_8, and 54 for C_4H_6) were obtained.
33. Pacchioni, G., and Lambert, R. M., *Surf. Sci.* **304**, 208 (1994).
34. Fahmi, A., and van Santen, R. A., *J. Phys. Chem.* **100**, 5676 (1996).
35. Burkart, S., Blessing, N., and Ganteför, G., *Phys. Rev. B* **60**, 15639 (1999).
36. Abbet, S., Sanchez, A., Heiz, U., Schneider, W.-D., Ferrari, A. M., Pacchioni, G., and Rösch, N., *Surf. Sci.* **454–456**, 984 (2000).
37. Roberts, C., Johnston, R. L., and Wilson, N. T., *Theor. Chem. Acc.* **104**, 123 (2000).